

Lidong ZHAO, Binyou FU, Dingyong HE, Pia KUTSCHMANN

Development of a new wear resistant coating by arc spraying of a steel-based cored wire

© Higher Education Press and Springer-Verlag 2009

Abstract In the present study, a cored wire of 304 L stainless steel as sheath material and NiB and WC-12Co as filler materials was designed and deposited to produce a new wear resistant coating containing amorphous phase by arc spraying. The microstructure of the coating was investigated. The porosity and hardness of the coating were determined. The wear performance of the coating was evaluated. The XRD and TEM analyses showed that there are high volume of amorphous phase and very fine crystalline grains in the coating. DTA measurements revealed that the crystallization of the amorphous phase occurred at 579.2°C. Because metallurgical processes for single droplets were non-homogenous during spraying, the lamellae in the coating have different hardness values, which lie between about 700 and 1250 HV_{100g}. The abrasive wear test showed that the new Fe-based coating was very wear resistant.

Keywords amorphous phase, arc spraying, microstructure, wear, cored wire

1 Introduction

Arc spraying is an established industrial coating process. The major advantages of arc spraying are low cost, high efficiency, simple operation and good mobility. Therefore, arc sprayed coatings have been widely used in various applications for wear and corrosion protection. To produce economical wear resistant coatings by arc spraying, steel

wires such as 3Cr13, 7Cr13, and Fe-based cored wires with carbides as main filler materials are usually applied.

Amorphous alloys are usually characterized by high strength, high hardness, superior corrosion and wear resistance [1,2]. Recently, a number of Fe-based amorphous alloys have been developed in Fe-Cr-B system [3]. The high hardness of the amorphous alloys gives a good inducement to develop new Fe-based wear resistant coatings based on the amorphous alloys. Our study aimed at developing of wear resistant coatings containing hard amorphous phase and fine crystallites. In the present study, a cored wire of 304 L stainless steel as sheath material and NiB and WC-12Co powders as filler materials were designed and deposited by arc spraying. The microstructure of the coating was investigated and the coating hardness was measured. The wear resistance against abrasives was evaluated in comparison with a conventional arc sprayed coating of 3Cr13.

2 Experimental

A cored wire in a diameter of 2.0 mm was used to produce coatings by arc spraying. The sheath material of the cored wire was 304 L stainless steel. A NiB powder (81.5% Ni, 18.0% B, 0.5% C; 150–250 μm; crushed) and a WC-12Co powder (15–45 μm; agglomerated and sintered) were employed as the filler materials in the cored wire. The mass ratio of the sheath material to the filler materials was 7:3. The nominal chemical composition of the cored wire (wt. %) was: 51.6% Fe, 25.7% Ni, 12.7% Cr, 5.0% W, 4.0% B, 0.7% Co, and 0.3% C. Grit-blasted steel samples (56 mm×25 mm×5 mm) were deposited by an arc spraying system JZY-250. The spray parameters were as follows: arc voltage, 32 V; arc current, 180 A; air pressure, 0.55 MPa; spray distance, 100 mm. About 1 mm thick coatings were produced.

The microstructure of the coating was investigated by means of optical microscopy and transmission electron microscopy (TEM). The transmission electron microscopy

Received October 30, 2008; accepted November 20, 2008

Lidong ZHAO (✉), Pia KUTSCHMANN
Surface Engineering Institute, RWTH Aachen University, Juelicher Str.
334a, Germany
E-mail: zhao@iot.rwth-aachen.de

Binyou FU, Dingyong HE
College of Materials Science and Engineering, Beijing University of
Technology, Beijing 100124, China

field images and selected area diffraction (SAD) patterns were obtained using JEM-2000FX TEM analytical electron microscope. The phase composition in the coating was analyzed using D8 ADVANCE X-ray diffractometer (XRD) by BRUKER/AKS, Germany. Porosity measurements were performed on cross sections of the coatings with an image analyzer. Ten measurements were conducted to get an average value. Differential thermal analysis (DTA) was conducted using the STA-449C unit with a heating and cooling rate of 20 K/min in nitrogen to determine the crystallization temperature of the amorphous phase in the coating. The microhardness of the coating was measured using a micro Vickers hardness tester MicroMet 1 by Buehler. The measurements were carried out on cross-sections of the coating with a 100 g load and 15 s dwell time.

Abrasive wear tests were carried out using a wet sand rubber wheel tester (Model MLS-225). The specimen dimension was 57 mm×25 mm×6 mm. Silica (224–355 μm) in a sharp, angular morphology were used as abrasives. A load of 100 N was applied on the contact surface between the coating and the rubber wheel. The rubber wheel peripheral speed was 240 rpm. The specimen was immersed in an abrasive mortar with a weight ratio of $W_{\text{silica}}:W_{\text{water}}$ of 3:2. The tests were performed with a pre-abrading of 1000 cycles and a refining abrading of 2000 cycles. The specimens were cleaned ultrasonically in an acetone bath for 3–5 minutes before and after testing. The weight loss of the specimens after testing was measured by a BS224S electronic balance. An arc sprayed 3Cr13 coating was tested for comparison.

3 Results

Figure 1 demonstrates the XRD pattern of an as-sprayed coating. A broad halo peak, centered on the diffraction angle of about 45°, can be seen, indicating that an amorphous phase exists in the coating. The volume content of the amorphous phase was calculated using the method based on comparing the area under the intensity curve of the X-ray scattered by the amorphous phase with the area under the original intensity curve [4]. The result shows that the volume content of the amorphous phase in the coating amounts to 49.2%. Besides the amorphous phase, crystalline phases are also identified in the coating. They are iron phase (Fe,Ni), intermetallic phases Fe-Cr and Ni₄W, boride Fe₂B, and oxide Fe₂O₃. The peaks of the crystalline phases are not incisive, indicating that the crystalline grains should be very fine. According to Scherrer formula [5], the grain size decreases as the full-width half-maximum (FWHM) increases. The calculated result shows that the grain sizes are in a range of 4–30 nm. As shown in Fig. 1, NiB and WC in the filler materials cannot be identified in the coating, indicating most of the filler materials were melted and dissolved in the

melted sheath material during spraying. The formation of the amorphous phase can be mainly attributed to two factors: firstly, the nominal composition of the designed cored wire is in the suitable range with high glass forming ability in Fe-Cr-B system [3] and secondly, droplets solidify very fast at cooling rates between 10⁶–10⁷ K/s [6]. The phases Fe-Cr, Fe₂B and Ni₄W did not exist in the cored wire. They formed just during solidification and cooling of droplets. The phase Fe₂O₃ resulted from oxidation of the droplets.

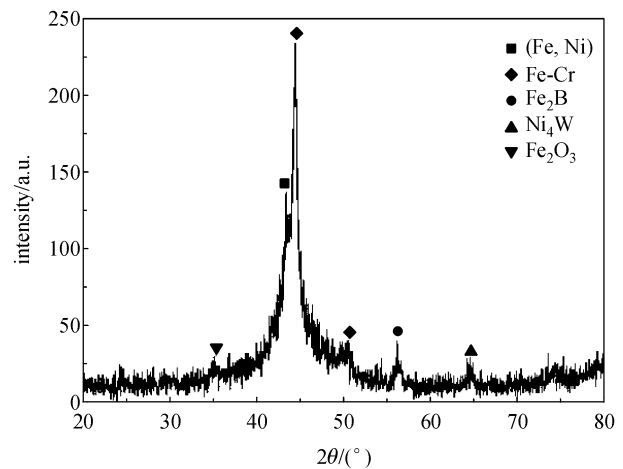


Fig. 1 XRD-pattern of as-sprayed coating

The thermal stability of the amorphous phase in the coating was evaluated using DTA measurements. Figure 2 shows the result of a DTA measurement with the as-sprayed coating during heating from room temperature to 900°C. The DTA measure curve of the as-sprayed coating reveals a solid-state phase transformation at 579.2°C. During cooling from 900°C to room temperature, no solid-state phase transformation could be detected. The same sample was then reheated up to 900°C after cooling to

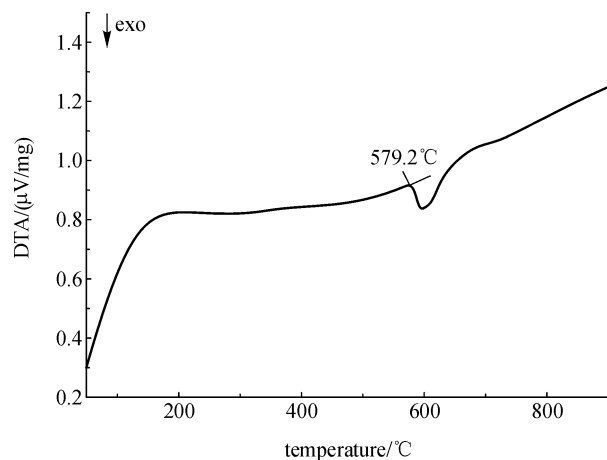


Fig. 2 DTA curve of as-sprayed coating during heating from room temperature to 900°C

room temperature. The phase transformation at 579.2°C did not occur this time. Therefore, it can be said that the phase transformation at 579.2°C is attributed to the crystallization of the amorphous phase in the coating.

An optical micrograph of a cross-section of the arc-sprayed coating is shown in Fig. 3. A typical lamellar structure can be seen, indicating that most of the atomized droplets were in molten or semi-molten state on impacting onto the substrate. Some pores are visible as dark contrast regions, but generally the coating has a dense layered structure. The measured porosity amounts to 2.7%. Figure 3 shows clear contrasts between single lamellae in the coating. The contrasts are attributed to differences in composition and hardness of the lamellae. The microhardness measurements on the lamellae proved this point. For example, the microhardness of light lamellae as marked at point *A* lies mostly between 700 and 800 $\text{HV}_{100\text{g}}$, while the grayish-white lamellae as marked at point *B* are much harder, having mostly a value between 850 and 1250 $\text{HV}_{100\text{g}}$. The differences in compositions and hardness of lamellae resulted from non-homogenous metallurgical processes within single droplets during spraying. Some droplets contained more dissolved filler materials, other droplets less. Besides, in single droplets a good homogenization could not be completely realized because of a very short duration from melting to solidification. TEM analysis was undertaken to obtain more detailed

information on the microstructure. As shown in Fig. 4, amorphous phase and nanocrystalline grains can be recognized. The diffraction pattern, shown in left bottom corner, shows the diffuse halo of amorphous phase. The diffraction pattern, shown in left top corner, proves a Fe-based crystalline phase.

The abrasive wear tests showed that the average mass loss of the cored wire coating was 0.1126 g, while the average mass loss of the 3Cr13 coating was 0.5967 g. The cored-wire coating exhibited an excellent abrasive wear resistance compared with the 3Cr13 coating. The morphology of the worn surfaces is shown in Fig. 5. As shown in Fig. 5(a), there are numerous deep plastic furrows on the worn surface of the 3Cr13 coating, indicating a typical micro-cutting mechanism for the wear. For the cored wire coating, plastic furrows can still be recognized. However, they are much shallower than those for the 3Cr13 coating. The harder lamellae with a microhardness of up to 1250 $\text{HV}_{100\text{g}}$ in the cored wire coating were responsible for shallower furrows, because they could strongly hinder in-cutting of silica particles.

4 Conclusions

In the present study, a cored wire of 304 L stainless steel as sheath material and NiB and WC-12Co powders as filler

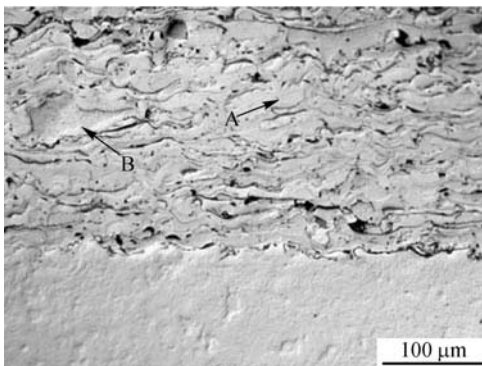


Fig. 3 Optical micrograph of cross-section of as-sprayed coating

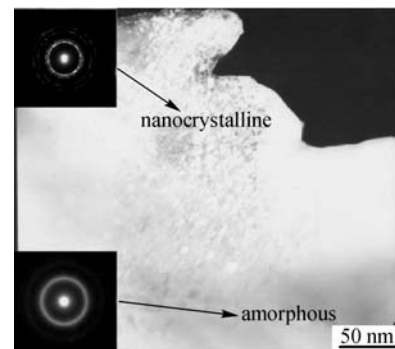


Fig. 4 TEM micrograph of as-sprayed coating

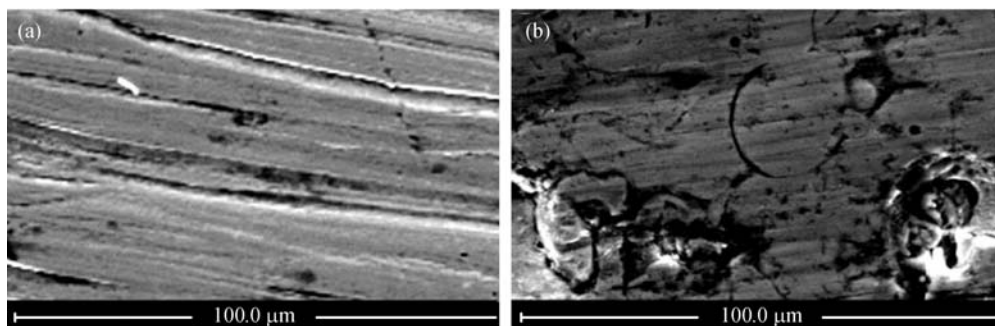


Fig. 5 Morphology of the worn surfaces. (a) 3Cr13 coating; (b) cored wire coating

materials was designed and deposited to produce a new wear resistant coating containing amorphous phase and very fine crystalline grains by arc spraying. About 1 mm thick coating was deposited. The arc sprayed coating shows a typical lamellar structure. The XRD and TEM analyses showed that there are amorphous phase and very fine crystalline grains in the coating. DTA measurements revealed that the crystallization of the amorphous phase occurred at 579.2°C. Because metallurgical processes for single droplets were non-homogenous, the lamellae in the coating have different hardness values, which lie between about 700 and 1250 HV_{100g}. The abrasive wear tests showed that the new cored wire coating is very wear resistant.

Acknowledgements The authors gratefully acknowledge the financial support of the German Science Foundation (DFG) within the scope of the project ZH205/1-1 for carrying out part of the study above reported.

References

1. Inoue A, Shen B L, Chang C T. Super-high strength of over 4000 MPa for Fe-based bulk glassy alloys in $[(\text{Fe}_{1-x}\text{Co}_x)_{0.75}\text{B}_{0.2}\text{Si}_{0.05}]_{96}\text{Nb}_4$ system. *Acta Mater*, 2004, 52, 4093–4099
2. Pang S J, Zhang T, Asami K, Inoue A. Synthesis of Fe-Cr-Mo-C-B-P bulk metallic glasses with high corrosion resistance. *Acta Mater*, 2002, 50, 489–497
3. Ponnambalam V, Poon S J, Shiflet G J. Fe-based bulk metallic glasses with diameter thickness larger than one centimeter. *J Mater Res*, 2004, 19, 1320–1324
4. Vainshtein B K. Diffraction of X-ray at chain molecules, M publ House AN SSSR, 1963
5. Klug H P, Alexander L E. *X-Ray Diffraction Procedures*, New York: Wiley, 1974
6. Moreau C, Cielo P, Lamontagne M, Dallaire S, Krapez J C, Vardelle M. Temperature evolution of plasma sprayed niobium particles impacting on a substrate. *Surf Coat Technol*, 1991, 46, 173–187